

THROUGH-SUPPORT-COUPLED MICROMECHANICAL FILTER ARRAY

Gavin K. Ho, Reza Abdolvand, and Farrokh Ayazi

School of Electrical and Computer Engineering, Georgia Institute of Technology

ABSTRACT

This paper presents a new concept for implementing high-order mechanically-coupled ultra-small bandwidth micro-mechanical filter arrays without using discrete coupling elements. Adjacent resonators are coupled by elastic deformation at the support, and filter bandwidth is defined by the spacing between resonating elements. We demonstrate a second-order through-support-coupled capacitively-transduced 1.72MHz 0.008%BW ($Q_{filter} \approx 12000$) bandpass flexural-mode beam filter array implemented on SOI. The coupling concept and experimental results were verified with finite element analysis using ANSYS. This integrated coupling technique does not introduce additional fabrication requirements for a discrete mechanical coupling element and therefore has strong potential for application to high-order higher frequency filter arrays. Resonator fine tuning is shown to be essential for obtaining ultra-small coupling-limited filter bandwidths.

1. INTRODUCTION

Recent developments in micromechanical resonators show strong potential for integration of these frequency selective components as bandpass filters in microsystems. Efforts are underway to obtain micromechanical resonators in the UHF band for application in mobile communications. The next task at hand is to implement highly-selective bandpass filters at these frequencies with percentage bandwidths (%BW) on the order of 0.01% ($Q_{filter} = 10000$). Various implementations of second-order coupled-resonator filter arrays have been demonstrated, with percentage bandwidths of 0.01% at 600kHz [1], 0.23% at 7.8MHz [2], and 0.7% at 68MHz [3]. Implementation of small percentage bandwidth micromechanical filter arrays at greater center frequencies is shown to be more challenging, and it defines the motivation for this work.

The resonance frequency for a single degree of freedom (SDOF) mechanical system is

$$\omega = 2\pi f = \sqrt{\frac{k_{eff}}{m_{eff}}} \quad (1)$$

where the effective mass m_{eff} and effective stiffness k_{eff} are evaluated at a particular point of interest. For a general homogeneous and continuous system,

$$m_{eff} = \rho \frac{\int \phi^2(x, y, z) dV}{\phi_c^2}, \quad k_{eff} = \omega^2 m_{eff} \quad (2)$$

where ρ is the density, $\phi(x, y, z)$ is the mode shape and ϕ_c is the modal displacement at the point (x_c, y_c, z_c) .

A second-order mechanical bandpass filter model containing two individual resonating elements and a

massless coupling spring k_c is shown in Fig. 1. The first resonance of this two degree of freedom (2DOF) system occurs with the resonators in-phase at frequency f_1 , corresponding to the natural frequency of the SDOF system expressed in (1). The second resonance of this 2DOF system occurs with the resonators out-of-phase at frequency

$$f_2 \approx f_1 \left(1 + \frac{k_c}{k_{eff}} \right) \quad (3)$$

for $k_{eff} \gg k_c$. Thus, the frequency separation Δf between the two resonance modes is determined by the ratio of the coupling stiffness to the effective stiffness of the resonator.

$$\Delta f = f_2 - f_1 \approx f_1 \frac{k_c}{k_{eff}} \quad (4)$$

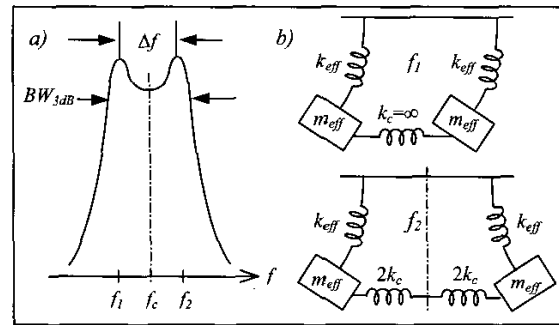


Figure 1: a) Frequency response of a second-order system, b) vibration modes of a discrete 2DOF mechanical system.

To reduce the frequency separation between the coupled modes, the coupling stiffness needs to be minimized while the resonator stiffness at the coupling location is maximized. Low frequency (<0.5MHz) mechanical filters employ compliant wires as coupling elements to provide small Δf [4]. Compliant coupling wires, however, are difficult to implement in high frequency micromechanical filters having small resonating structures. Hence, novel resonator coupling methods are required. From (2), the maximum k_{eff} is obtained at a low-velocity point, where there is small modal displacement. Placement of discrete coupling elements at low-velocity points have demonstrated less than 1% bandwidths up to 68MHz [3], but extension of this approach to higher frequencies and smaller bandwidths require smaller coupling elements that have additional fabrication demands. Capacitively-coupled resonator arrays [1] alleviate these fabrication challenges, but small coupling capacitances (in the range of 10-100fF for UHF resonator coupling) are required, and coupling strength may be affected by parasitics. Therefore, alternative coupling techniques need to be considered for implementing high-order VHF and UHF highly-selective bandpass filters.

2. CONCEPT

To further reduce the effective stiffness at the coupling location, the low-velocity concept is extended. In structural analyses, clamped boundaries are commonly assumed as ideal (i.e., infinitely rigid). However, solids are elastic with a finite stiffness. Any deviation from the equilibrium position will cause displacement at these elastic clamped boundaries. This finite stiffness and small non-zero displacement enables resonators to be coupled through the support.

In this work, we exploit the elasticity of the support medium to provide coupling between adjacent resonators. Using this integrated coupling technique, there are no additional fabrication requirements for a discrete coupling element; attainment of higher frequency filter arrays is only limited by the ability to fabricate the dimensionally smaller resonators.

We demonstrate this technique using arrays of clamped-clamped flexural beam resonators, where the fundamental natural frequency of a beam of length L and thickness t , assuming infinitely rigid boundaries, is:

$$f_i = 1.027 \frac{t}{L^2} \sqrt{\frac{E}{\rho}} \quad (5)$$

A simple one-dimensional lumped-parameter model of through-support coupling is shown in Fig. 2. The elastic support is modeled with springs k_s and k_c for the support stiffness and coupling stiffness respectively. The coupling spring stiffness is a function of the spacing between the resonators δ . If modeled as an axially-loaded member, the stiffness k_c with an effective width w_{eff} and height h , is:

$$k_c = \frac{EA}{L} = \frac{Ew_{eff}h}{\delta} \quad (6)$$

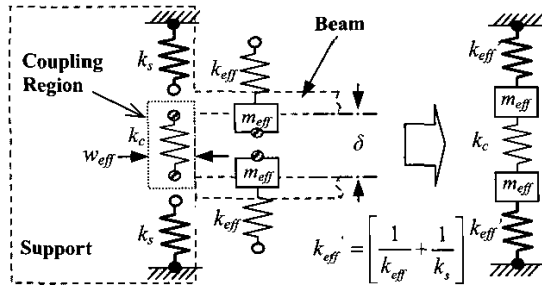


Figure 2: Discrete mechanical model of through-support coupling in a two-resonator array.

From (6), the coupling stiffness is inversely proportional to the spacing δ between the beams. Thus, we expect to have smaller frequency separation Δf for beams placed further apart. We approximate the coupling region as massless and assume the support compliance $1/k_s$ is small and negligible.

3. EXPERIMENTATION

Various capacitively-transduced beam resonator arrays were fabricated on SOI wafers with a $10\mu\text{m}$ thick single crystal silicon (SCS) n-type low-resistivity (100) device layer, a $2\mu\text{m}$ thick buried oxide (BOX) layer, and a $450\mu\text{m}$ thick low-resistivity handle layer. The simple coupling technique enabled the devices to be defined entirely with one lithography mask and deep reactive ion etching (DRIE). These in-plane flexural mode beams were aligned to the $\langle 110 \rangle$ direction, which has a directional stiffness of 168GPa .

The fabricated devices include second-, third-, and fourth-order arrays of clamped-clamped beam resonators with $L \times t$ dimensions of $100\mu\text{m} \times 2\mu\text{m}$ (Fig. 3) and $500\mu\text{m} \times 4\mu\text{m}$ with $1\mu\text{m}$ capacitive gaps. The calculated fundamental natural frequencies of these $100\mu\text{m} \times 2\mu\text{m}$ and $500\mu\text{m} \times 4\mu\text{m}$ beams using (5), are 1.74MHz and 140kHz respectively ($\rho = 2328\text{kg/m}^3$). SOI fabrication technology enabled the coupling region (see Fig. 2) to be isolated from the handle by ensuring sufficient oxide removal beneath the support. The devices were released in HF solution for $30\mu\text{m}$ of oxide undercut.

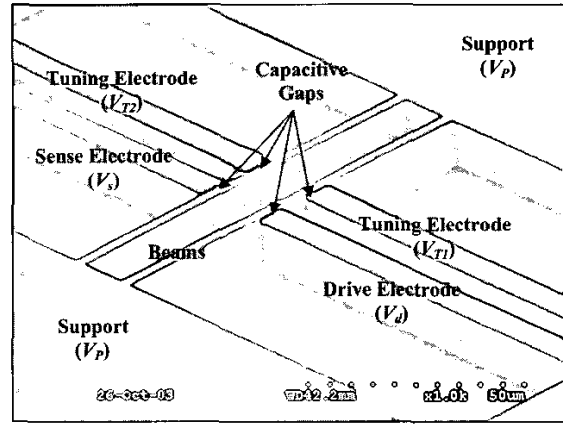


Figure 3: SEM of an array of two $100\mu\text{m} \times 2\mu\text{m}$ clamped-clamped beams with $9\mu\text{m}$ spacing.

In order to obtain a predictable filter response, resonators with identical individual resonant frequencies are required in the array. Therefore, compensation for fabrication non-idealities is necessary [5]. Electrostatic tuning provides an equivalent electrical stiffness that decreases the overall stiffness, and hence frequency, of a resonator. For a non-ideal two-resonator array, the electrostatic tuning voltage $\Delta V_i = V_P - V_{Ti}$ is applied to the higher frequency resonator. The tuning electrode of the alternate resonator is polarized at V_P (i.e. $\Delta V = 0$). The devices are wire-bonded on a PCB and tested in high vacuum ($\sim 5\mu\text{Torr}$) in a custom-fabricated stainless steel vacuum chamber with coaxial feedthroughs.

Second-Order Arrays

A large number of second-order filter arrays with $100\mu\text{m}$ long, $2\mu\text{m}$ thick beams with different spacing were tested. Large 100V polarization voltages V_P were necessary because of the large $1\mu\text{m}$ capacitive gaps. The frequency response of the device in Fig. 3 shows two distinct resonance peaks in high vacuum near 1.72MHz , each with quality factor Q of 25000, with a tuned Δf of 650Hz (Fig. 4a). A similar device with $18\mu\text{m}$ beam spacing showed a filter response at 1.72MHz with 140Hz 3dB bandwidth ($0.008\%\text{BW}$), less than 1dB ripple and 40dB out-of-band rejection (Fig. 5a). Measurement data for second-order $100\mu\text{m}\times 2\mu\text{m}$ beam arrays is summarized in Table 1, and shows that the coupling-limited (tuned) frequency separation decreases with increased beam spacing.

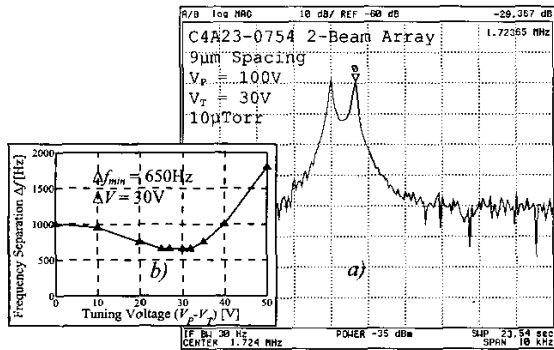


Figure 4: a) Frequency response and b) tuning characteristic of an array of two $100\mu\text{m}\times 2\mu\text{m}$ beams with a beam spacing of $9\mu\text{m}$.

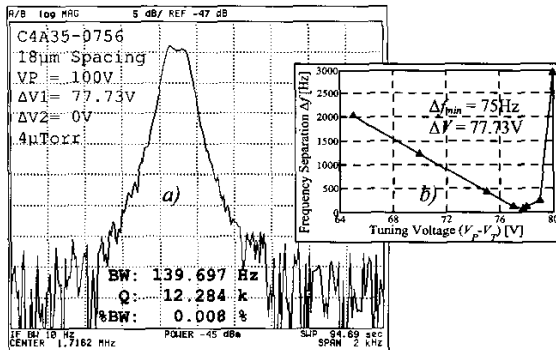


Figure 5: a) Frequency response and b) tuning characteristic of an array of two $100\mu\text{m}\times 2\mu\text{m}$ beams with a beam spacing of $18\mu\text{m}$.

Table 1: Measurement data for arrays of two $100\mu\text{m}\times 2\mu\text{m}$ clamped-clamped beams ($V_P=100\text{V}$).

Spacing δ [μm]	f_c [MHz]	Δf (With Tuning) [Hz]	Tuning V $\Delta V = V_P - V_T$ [V]
3	1.715	2400	78.0
6	1.691	900	50.0
9	1.724	650	30.0
18	1.716	75	77.73

The tuning characteristic of the device in Fig. 3 has a minimum Δf at a tuning voltage difference ΔV_1 of 30V at one electrode with $\Delta V_2=0$ at the other electrode (Fig. 4b). The two-beam array with $18\mu\text{m}$ spacing was finely tuned with ΔV_1 of 77.73V to obtain minimal frequency separation of 75Hz (Fig. 5b). A higher tuning voltage was required because the non-uniformity of the beams is greater in this device. The tuning curves indicates that this form of tuning acts only to match resonators since a minimum frequency separation is achieved at only one particular voltage.

High-Order Arrays

Large arrays of coupled resonators provide high-order filters with greater selectivity. Through-support coupling can be extended to larger arrays simply by placing more beams adjacent to each other. Four $500\mu\text{m}\times 4\mu\text{m}$ clamped-clamped arrayed beams with $9\mu\text{m}$ spacing are shown in Fig. 6a.

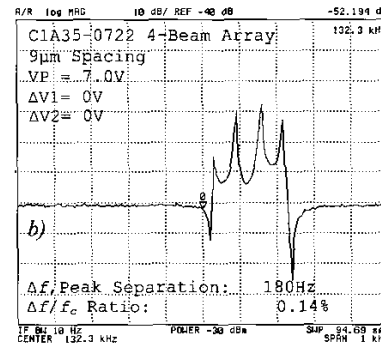
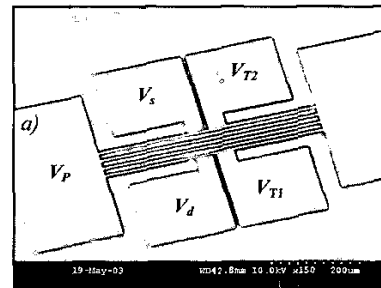


Figure 6: a) SEM of a four-resonator array of $500\mu\text{m}\times 4\mu\text{m}$ beams with $9\mu\text{m}$ spacing, b) frequency response of the array.

In this four-resonator array, only the external beams experience the subtractive electrical stiffness, causing non-uniformity in the array. Nonetheless, a frequency response with four evenly spaced peaks 60Hz apart with $f_c=132.5\text{kHz}$ was obtained at a polarization voltage V_P of 7V with both $\Delta V=0$ (Fig. 6b). In this electrode configuration, the peak separation and mode order shifted significantly with changes in V_P . Therefore, alternative configurations are necessary to achieve predictable characteristics for arrays containing more than two beams.

4. FINITE ELEMENT MODELING

A three-dimensional anisotropic finite element (FE) model was created to predict the interaction at the support of second-order SCS beam filter arrays. The model includes the beams, $200\mu\text{m}\times 200\mu\text{m}$ square supports, and buried oxide layer with $30\mu\text{m}$ undercut. The structure is constrained in all DOF at the bottom of the buried oxide. The harmonic and modal analysis results for $100\mu\text{m}\times 2\mu\text{m}$ beams with $\delta=18\mu\text{m}$ (Fig. 7) show two resonances centered at 1.71MHz with Δf of 96Hz . Interestingly, ANSYS indicates that the beams resonate out-of-phase in the lower frequency mode and are in-phase in the higher frequency mode. The interaction at the support, plotted as displacement in the y-direction in Fig. 8, shows that the spring k_s has different contributions in the two modes. This interaction is most likely the cause of the switched modes. The FE results also show that the integrated coupling element is loaded axially in the out-of-phase mode, (indicated by the changing contours in Fig. 8a), and has negligible deformation (uniform y-displacement contours in Fig. 8b) when the resonators are in-phase.

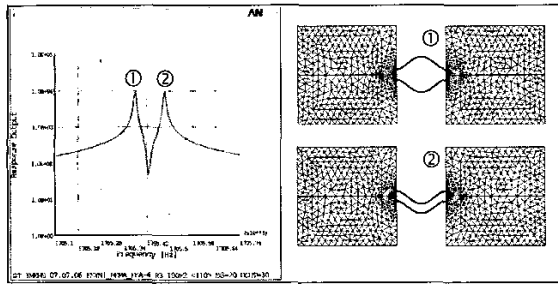


Figure 7: ANSYS finite element harmonic and modal analysis results for an array of two $100\mu\text{m}\times 2\mu\text{m}$ beams.

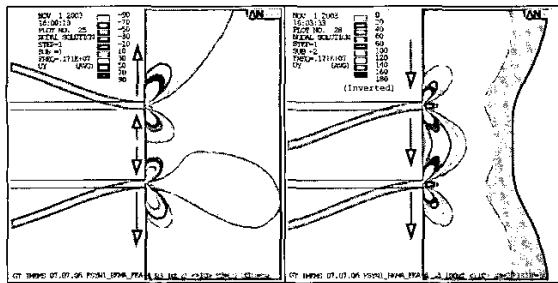


Figure 8: Interaction at the support of a $100\mu\text{m}\times 2\mu\text{m}$ array with $18\mu\text{m}$ spacing in the a) first mode and b) second mode.

Experimental data, ANSYS modal analysis results, and a δ^{-1} curve fit are plotted in Fig. 9 to observe the effect of beam spacing on frequency separation. At small beam spacing, the experimental data of Δf is slightly greater than FEA results. The beam-support interfaces, when carefully inspected with SEM, were found to have rounded corners that cause increased coupling stiffness and leads to greater Δf . The rounded corners have less effect for larger beam spacing. At large δ , however, the experimental Δf are slightly lower than predicted by ANSYS. Large spacings, having low coupling

stiffness, require precise modeling of boundary conditions for accurate results. The assumed boundary conditions of the BOX caused a minor increase of coupling stiffness in the FE model, leading to greater predicted Δf for $\delta=18$.

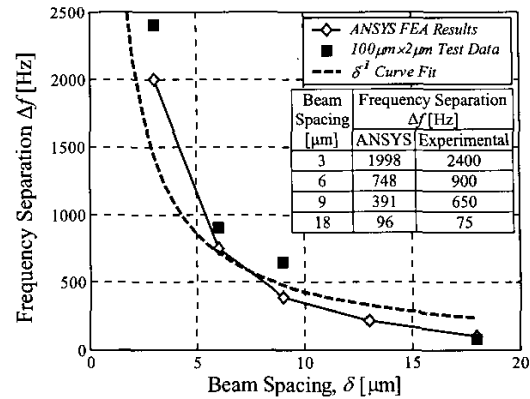


Figure 9: Frequency separation Δf vs beam spacing for two $100\mu\text{m}\times 2\mu\text{m}$ clamped-clamped beams ($f_c \approx 1.71\text{MHz}$).

5. CONCLUSION

We demonstrated that coupling of adjacent resonators can be provided by the elastic support medium to implement topographically-simple filter arrays with very small percentage bandwidths. The coupling-limited filter bandwidth was shown to be defined primarily by resonator spacing at the supports. Through-support-coupling enabled a second-order filter with a center frequency of 1.72MHz and filter Q of 12000 ($0.008\% \text{BW}$) from an array of two $100\mu\text{m}\times 2\mu\text{m}$ clamped-clamped beams. This technique was also shown to be extendable to larger arrays. The importance of individual resonator fine tuning was demonstrated to be especially important in implementing ultra-small percentage-bandwidth filters. Implementation of high-order matched resonator arrays and further investigation in elastic support interaction is currently underway.

ACKNOWLEDGEMENTS

The authors thank the cleanroom staff of the Georgia Tech Microelectronics Research Center for their assistance. This work was funded under DARPA contract #DAAH01-01-1-R004.

REFERENCES

- [1] S. Pourkamali, R. Abdolvand and F. Ayazi, *MEMS 2003*, pp.702-705.
- [2] F. D. Bannon, III, J. R. Clark, and C. T.-C. Nguyen, *IEEE JSSC* V35, N4, Apr 2000, pp. 512-526.
- [3] A. C. Wong, J. R. Clark, and C. T.-C. Nguyen, *Transducers '99*, pp.1390-1393.
- [4] R. A. Johnson, *Mechanical Filters in Electronics*, Wiley: New York, 1983, pp115.
- [5] Q. Jing, H. Luo, T. Mukherjee, L. R. Carley, and G. K. Fedder, *MEMS 2000*, pp.187-192